

Transit timing variations in the HAT-P-13 planetary system

András Pál^{1,2*†}, Krisztián Sárneczky¹, Gyula M. Szabó^{1,3}, Attila Szing¹,
László L. Kiss^{1,4}, György Mező¹ and Zsolt Regály¹

¹ Konkoly Observatory of the Hungarian Academy of Sciences, Konkoly Thege Miklós út 15-17, Budapest, H-1121, Hungary,

² Department of Astronomy, Loránd Eötvös University, Pázmány Péter sétány 1/A, Budapest H-1117, Hungary,

³ Department of Experimental Physics and Astronomical Observatory, University of Szeged, 6720 Szeged, Hungary

⁴ Sydney Institute for Astronomy, School of Physics A28, University of Sydney, NSW 2006, Australia

Accepted ..., Received ... ; in original form ...

ABSTRACT

In this Letter we present observations of recent HAT-P-13b transits. The combined analysis of published and newly obtained transit epochs shows evidence for significant transit timing variations since the last publicly available ephemerides. Variation of transit timings result in a sudden switch of transit times. The detected full range of TTV spans ≈ 0.015 days, which is significantly more than the known TTV events exhibited by hot Jupiters. If we have detected a periodic process, its period should be at least ≈ 3 years because there are no signs of variations in the previous observations. This argument makes unlikely that the measured TTV is due to perturbations by HAT-P-13c.

Key words: planetary systems – stars: individual: HAT-P-13 – techniques: photometric

1 INTRODUCTION

Transit timing variations (TTVs) of transits are expected in transiting extrasolar planetary systems where the host star has more than one companion. This effect might reveal the presence of other companions with smaller masses (see e.g. Agol et al. 2005; Steffen & Agol 2007) or co-orbital bodies as well (Ford & Holman 2007). On the other hand, if the system has two or more known planetary components, the magnitude of the TTV effects can be predicted and/or used to characterize the system more precisely (Holman et al. 2010; Steffen et al. 2010). Similarly, the lack of TTVs can rule out other companions above a certain limit (Csizmadia et al. 2010). One should note that even two-body systems (i.e. the parent star and the planet) can show significant TTVs due to non-gravitational physical processes (see e.g. Fabrycky 2008) and in the case of eccentric orbits, there are intrinsic timing variations due to the effects of general relativity (see e.g. Pál & Kocsis 2008). In the case of two planetary companions, the magnitude of the TTV effects can be predicted analytically using the same methodology that is known for hierarchical stellar systems (Borkovits et al. 2003), and of course, by numerical integrations.

At the time of its discovery, the planetary system or-

biting the star HAT-P-13 was the only known multiple extrasolar planetary system that exhibits at least one transiting planet as well (HAT-P-13b, Bakos et al. 2009). Follow-up studies showed that the host star has a spin alignment with respect to the orbital plane of the transiting planet (Winn et al. 2010) as well as this work also noticed a significant long-term drift in the radial velocity of the host star that might be interpreted as a presence of a third companion. Additional studies (Szabó et al. 2010) reported the lack of primary transits of the long-period second companion HAT-P-13c, and presented additional observations from the transits of the close-in planet as well. As of this writing, no other (than Bakos et al. 2009; Szabó et al. 2010) publicly available photometric data are available for this planetary system. Here we describe recent photometric measurements of the host star. The analysis of the light curves showed significant timing variations since the last public ephemerides. The structure of this Letter is as follows. In Section 2 we describe details of the observations, data reduction and light curve modelling. The analysis of the results yielded by light curve fits is presented in Section 3. Section 4 discusses possible scenarios for the observed TTVs and summarizes our results.

* E-mail address: apal@szofi.net

† Bolyai Fellow

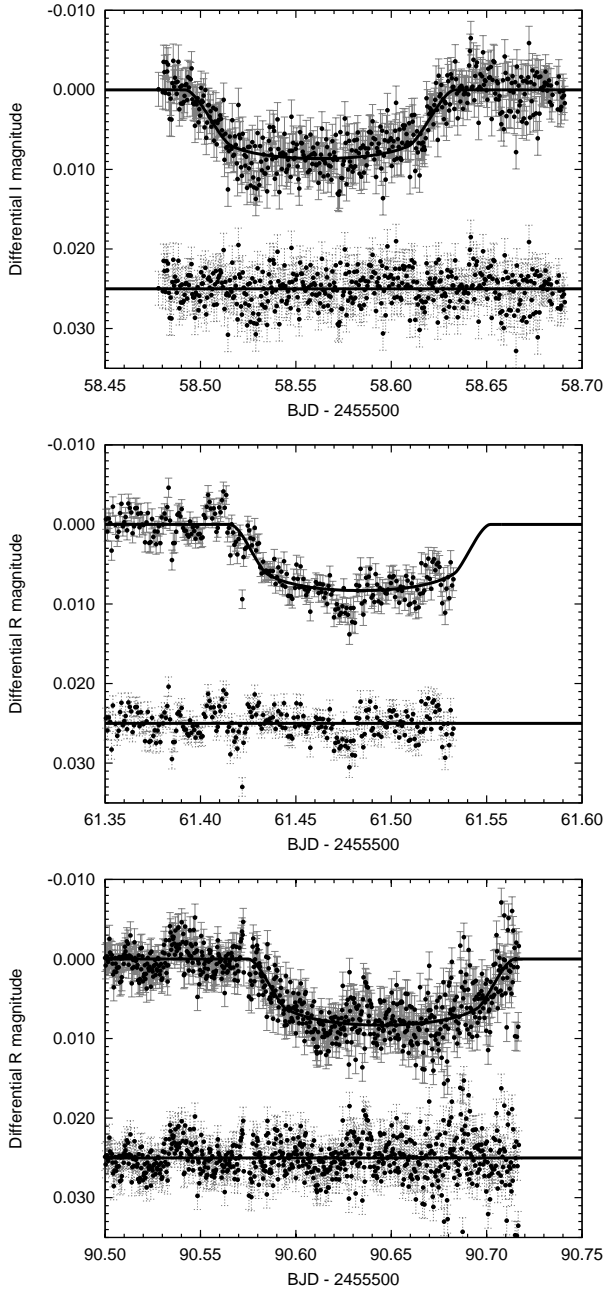


Figure 1. Photometry of the star HAT-P-13 on the nights of 2010 December 27/28 (upper panel), December 30/31 (middle panel) and 2011 January 28/29 (lower panel), using the facilities of the Piszkéstető Mountain Station, Konkoly Observatory. Superimposed are the best-fit transit model light curves. Below the light curve plots, the fit residuals are also shown. See text for further details.

2 OBSERVATIONS AND DATA REDUCTION

We carried out photometric observations of the star HAT-P-13 with the telescopes of the Konkoly Observatory, located at the Piszkéstető Mountain Station on three separate nights. On the night of 2010 December 27/28, we used the 60/90/180 cm Schmidt telescope, equipped with an Apogee ALTA-U 4k × 4k CCD camera. The following two events, on the night of December 30/31 and 2011 Jan-

uar 28/29 has been partially observed (due to weather circumstances on December 30 and due to dawn twilight on January 28) with the 100 cm Ritchey-Chrétien-Coudé (RCC) telescope equipped with a Princeton Instruments VersArray 1.3k × 1.3k camera. These setups of optics and cameras yielded a square-shaped field-of-view with a size of 1.17 and 0.11 degrees, for the Schmidt and RCC telescopes, respectively. At the first night we used Bessel I filter and an exposure time of 20 seconds (42 seconds cadence) while in the second and third night we used Cousins R filter and an exposure time of 60 and 25 seconds, respectively (here the readout time is relatively short, so this can be used as a cadence as well and on the last night the seeing was much better hence the shorter exposure time).

In the following we describe the data reduction processes and some aspects of the light curve modelling.

2.1 Data reduction

Reduction of raw technical and scientific frames has been carried out with the pipelines built on the software package described in Pál (2009). The calibration procedure followed the standard way of dark subtraction and flat-field corrections using dark frames taken with similar exposures as the scientific images. (employing the tasks `ficalib` and `ficombe`). The source identification, astrometric solution and centroid coordinates were derived as follows. First, individual point-like sources were extracted from each frame using the task `fistar`. These lists of profile coordinates were then cross-matched (Pál & Bakos 2006) between the frames and a reference frame, yielding both a list of matched pairs and the spatial transformation between two images. The polynomial order of the spatial transformation were 3 and 1 for the Schmidt and RCC fields, respectively (increasing these orders did not decrease the unbiased fit residuals). Then, using these initial differential astrometric solutions, the stellar pixel coordinates were refined using an independent profile centroid fit (done by the task `fiphot`) for the expected positions. These lists of refined profile coordinates were used to refine the spatial transformation as well. This is a rather relevant step because the point matching task (`grmatch`) sometimes misses a point and the exclusion of even a single point can yield a systematic deviation in the transformation coefficients whose error can propagate into the photometry errors (resulting in unexpected red noise). Following this two-stage astrometry, these refined coefficients were used to transform the reference object list to the system of individual frames to perform aperture photometry. Involving the task `fiphot`, aperture photometry was performed with annuli of appropriate sizes and a series of apertures from which we picked the best one later on the modelling. Differential magnitudes were then computed from these raw instrumental magnitudes using several nearby comparison stars. The white-noise uncertainties of the individual photometric points were derived from the photon noise, background noise and scintillation (Young 1967) noise components of both the target star and comparison stars.

2.2 Light curve modelling

Light curves obtained by the procedure (as described above) have been used to model the transit event and derive the respective parameters. In order to fit a model light curve to the observed data, we employed the analytic formulae of Mandel & Agol (2002). The effects of stellar limb darkening have been taken into account by fixing the quadratic limb darkening coefficients using the stellar atmospheric parameters (Bakos et al. 2009). These coefficients have been derived from the tables of Claret (2000). Since many of the regression methods used by us require the knowledge of parametric derivatives of the model function, we used the formulae provided by Pál (2008) to compute these partial derivatives.

The light curve models have been parameterised using $p \equiv R_p/R_*$, the planet-to-star size ratio, b^2 , the square of the impact parameter, the quantity ζ/R_* , related to the duration of the transit as $\zeta/R_* = 2/(T_{3.5} - T_{1.5})$ and $T_c = (T_{1.5} + T_{3.5})/2$, the time instance at the center of the transit (here $T_{1.5}$ and $T_{3.5}$ denotes the time instances when the center of the planet disc intersects the limb of the star inwards and outwards, respectively). See also Pál (2008) for further details on the advantages of this parameterisation. In addition to these parameters, we fitted simultaneously the out-of-transit magnitude, a linear trend in the out-of-transit magnitude (correcting to the effects of changing airmasses) and a linear decorrelation parameter against the variations resulted by the changes in the profile FWHM. In the case of the observation on 2010 December 30/31, we kept R_p/R_* , b^2 and ζ/R_* fixed, since this light curve does not cover the entire transit event. We employed the Markov Chain Monte Carlo method (MCMC; see Ford 2004) to obtain the *a posteriori* distribution of the fit parameters from which the best fit values, uncertainties and correlations can easily be derived. The best fit values for the light curve shape parameters for the event 2010 December 27/28 are $R_p/R_* = 0.0880 \pm 0.0031$, $b^2 = 0.544 \pm 0.086$ and $\zeta/R_* = 17.07 \pm 0.28$. These values agrees well with the previously published ones (Bakos et al. 2009). Fig. 1 shows the light curves with these best fit model functions superimposed while the best fit values for the transit center instances are listed in Table 1. This table also lists the previously published individual transit event instances as well, from Bakos et al. (2009) and Szabó et al. (2010). The fit residuals has been compared to the expected residual value that can be computed from the photon noise, background noise and scintillation of the star. We find that the fit residuals for the observation of 2010 December 27/28 were only larger by a factor of 1.05, that indicates a very good quality light curve with small systematic variations (red noise). Indeed, even the raw instrumental magnitudes (i.e. the magnitude of the target star without subtracting any comparison star) varied in a range of only 0.02 mag. However, the analysis of the observation from 2010 December 30/31 yielded a fit residual that is larger by a factor of ≈ 2 than the expected and as it clear from the lower plot on Fig. 1, the residuals contain significant amount of red noise. This was due to both weather circumstances and significant flat field image structures in the vicinity of HAT-P-13. Therefore we conservatively scaled up the derived errors by that factor of 2 (and this is the value that has been reported in Table 1). The observation carried out on 2011 January 28/29

Table 1. Transit center instances from previous works and recent measurements. Data for the events $-68 \dots +62$ are available from Bakos et al. (2009), for the events 124 and 161 data are taken from Szabó et al. (2010). The last three fields are the new measurements presented in this Letter. The event enumeration is from the same reference epoch as in Bakos et al. (2009). See text for further details.

Event	BJD	Error
-68	2454581.62406	0.00122
-1	2454777.01287	0.00100
0	2454779.92953	0.00063
1	2454782.84357	0.00155
24	2454849.92062	0.00075
35	2454882.00041	0.00150
62	2454960.73968	0.00178
124	2455141.55220	0.00100
161	2455249.45080	0.00200
267	2455558.56265	0.00098
268	2455561.48379	0.00400
278	2455590.64486	0.00179

was partial: the out-of-transit part of the light curve after the transit was not measured, however, the observed egress can be incorporated into the light curve analysis. This fit has been done similarly as for the night of December 27/28 and yielded $R_p/R_* = 0.0820 \pm 0.0078$, $b^2 = 0.471 \pm 0.214$ and $\zeta/R_* = 16.88 \pm 0.48$. These values also agrees well (within uncertainties) both with the fit of December 27/28 data and the published values. For the center of the transit, we obtain the value found in Table 1. For this analysis, the uncertainties yielded by the MCMC fit have been multiplied by 1.5 in order to take into account the red noise components: this value is the ratio of the fit residuals and the expected formal photometric errors (those have been derived from the photon and background noise and the scintillation). The uncertainties reported above for the geometric parameters and listed in Table 1 are these increased values.

3 TIMING VARIATIONS

Using the data of Bakos et al. (2009) and Szabó et al. (2010), the subsequent observed transit events can be modelled easily with a strictly periodic assumption: the formal errors reported in these papers yield an unbiased residual of $\chi_0 = 9.2$ for these 7 degrees of freedom. By defining the event $N_{tr} = 0$ as the reference epoch, this linear model yields $E = 2454779.92978 \pm 0.00049$ (BJD) and $P = 2.9162953 \pm 0.0000085$ days while $\text{Corr}(E, P) = -0.406$. These ephemerides gives an uncertainty of $\Delta t = 0.0021$ days for the predictions of the discussed events ($N_{tr} = 267, 268$ and 278 for the nights 2010 December 27/28, 30/31 and January 28/29). As it is clear from Fig. 2, these three recent measurements outlie from the linear fit by $8.4\text{-}\sigma$, $3.3\text{-}\sigma$ and $5.5\text{-}\sigma$, respectively. We note here that the significance of the first (December 27/28) measurement is determined mostly by the uncertainty of the predictions while the significance of the second one is determined by the uncertainty of that particular measurement. All in all, both values can be treated as a significant deviation.

Due to the significance of the results, i.e. the deviance of the transit center instances from the predictions, we applied

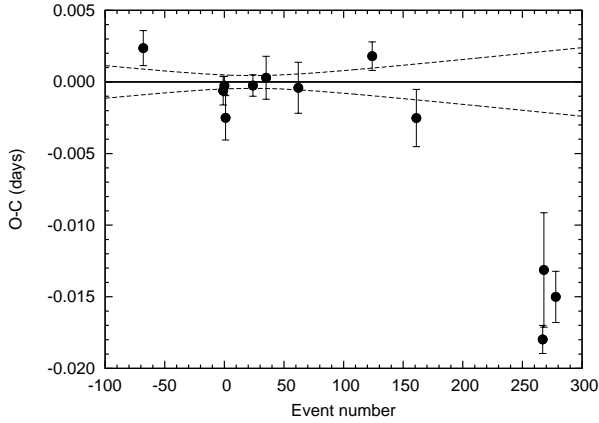


Figure 2. Transit timing variations as the function of the event number (cycles since event at the night of 2008 November 9/10). The points with the errorbars represent the individual measurements and the respective uncertainties as listed in Table. 1. The thick solid line is the best fit linear ephemerides to the first 9 data points while the thinner dashed lines above and below it represents the $1\text{-}\sigma$ errorbars of the best linear fit.

several independent analysis methods. These methods include the minimisation algorithm based on the downhill simplex method (Press et al. 1992), as well as a one-parameter scan. In the latter test, the light curve shape parameters (R_p/R_* , b^2 and ζ/R_*) have been fixed and only the T_c has been varied while the out-of-transit magnitude and other decorrelation parameters (see above) have been minimised using the classic linear least squares method. Additionally, we compared the statistical covariances with the covariances yielded by linear error propagation analysis. All of these methods have confirmed the results and uncertainties of the Markov Chain Monte Carlo analysis presented in the previous section. In addition to these tests, we checked other data acquisition logs to exclude other sources of possible systematic effects. The filesystem metadata information has been compared with the FITS keywords as well as the logs of the NTP daemon were also checked (this showed an approximately 0.002 seconds of standard deviation from the time synchronization servers).

4 DISCUSSION

There are a few examples for extrasolar planets proven to exhibit TTV. WASP-3b has been found to display a full TTV amplitude of 0.004 day period. As an explanation, a third planet has been inferred on a resonance orbit that may be either an inner or outer perturber (Maciejewski et al. 2010a). The TTV of WASP-5 is about 0.0023 day, and a set of different perturber solutions were invoked that can equivalently well explain the observed TTV (Fukui et al. 2010). WASP-10 exhibits a similar TTV to that of WASP-3 and WASP-5, its TTV has a full amplitude of 0.002 day with 5.47 day period. The perturber has been suggested to have $5 M_J$ mass and orbit in 5 : 3 mean motion resonance with WASP-10b (Maciejewski et al. 2010b). Other sources than perturbing planets are also known as sources of TTV, such as exomoons orbiting the planets (Szabó et al. 2006;

Simon, Szatmáry & Szabó 2007). However, the transit timing variations are in the order of a few seconds/minutes in the case of plausible moons, and the measured TTV of HAT-P-13b is not compatible with this predicted TTV amplitude.

The detected $O - C$ of HAT-P-13b is in the order of 0.01 days, significantly more than that of WASP-3, WASP-5 or WASP-10. Kepler-9b,c represent an example for such large TTV amplitude exhibited by Neptunes that orbit in strong resonance (Holman et al. 2010). However, HAT-P-13b is not very similar to the case of Kepler-9b,c. The planets in the Kepler-9 system exhibit a continuous variation of TTV with a period of few hundred days, while HAT-P-13b seemed to lack TTV during the first three years of follow-up observations, and then a sudden switch of TTV is observed.

This observed behaviour and the TTV amplitude of HAT-P-13b may be explained by perturbations by long period planets on non-resonant orbits. For instance, in Borkovits et al. (2010), a model planet similar to CoRoT-9 exhibits a large switch in $O - C$ of the inner planet in less than 1 year. Assuming an outer perturber of $5 M_J$ mass, 10,000 day orbital period and $e = 0.7$ eccentricity, the predicted amplitude results to be 0.013 days (see Fig. 6 in the cited paper). This value is quite similar to the $O - C$ variation that we report for HAT-P-13, suggesting that perturbations on the time-scale of the orbital period of a long-period perturber can explain our inferred TTV of HAT-P-13b. The detailed modeling is beyond the information content of the currently available dataset: there would be at least 6 orbital parameters to explain with the amplitude and the timing of the switch of the $O - C$ diagram, leading to a highly unconstrained problem. It may be unlikely that we observed perturbations of HAT-P-13c, because this non-resonant perturber would lead to TTV variations with 428.5 day amplitude and additional secular components. This period is covered by the current dataset and there are no signs for this period in the deduced TTV. Eventually, the most urgent task is deriving the period of the TTV shown by HAT-P-13b before predictions can be given to the nature of the perturber.

ACKNOWLEDGMENTS

The work of A. P. has been supported by the ESA grant PECS 98073 and by the János Bolyai Research Scholarship of the Hungarian Academy of Sciences. This project has also been supported by the “Lendület” Young Researchers Program of the Hungarian Academy of Sciences and the Hungarian OTKA Grants K76816, K83790, and MB08C 81013.

REFERENCES

- Agol, E., Steffen, J., Sari, R., & Clarkson, W. 2005, *MNRAS*, 359, 567
- Bakos, G. Á. et al. 2009, *ApJ*, 707, 446
- Borkovits, T., Érdi, B., Forgács-Dajka, E. & Kovács, T. 2003, *A&A*, 398, 1091
- Borkovits, T., Csizmadia, Sz., Forgács-Dajka, E. & Hegedüs, T. 2011, *A&A*, accepted (arXiv:1010.0884)
- Claret, A. 2000, *A&A*, 363, 1081
- Csizmadia, Sz. et al. 2010, *A&A*, 510, A94

- Fabrycky, D. 2008, ApJ, 677, 117
- Ford, E. 2004, AJ, 129, 1706
- Ford, E. B. & Holman, M. J. 2007, ApJ, 664, 51
- Fukui, A. et al. 2010, PASJ, accepted (arXiv:1009.5769)
- Holman, M. J. et al. 2010, Science, 330, 51
- Howard, A. W. et al. 2010, ApJ, submitted (arXiv:1008.3898)
- Maciejewski G. et al. 2010a, MNRAS, 407, 2625
- Maciejewski G. et al. 2010b, MNRAS, accepted (arXiv:1009.4567)
- Mandel, K. & Agol, E. 2002, ApJ, 580, L171
- Pál, A., & Bakos, G. Á. 2006, PASP, 118, 1474
- Pál, A. 2008, MNRAS, 390, 281
- Pál, A. & Kocsis, B. 2008, MNRAS, 389, 191
- Pál, A. 2009, PhD thesis (arXiv:0906.3486)
- Press, W. H., Teukolsky, S. A., Vetterling, W.T., Flannery, B.P., 1992, Numerical Recipes in C: the art of scientific computing, Second Edition, Cambridge University Press
- Simon, A. E., Szatmáry, K. & Szabó, Gy. M. 2007, A&A, 470, 727
- Steffen, J. H. & Agol, E. 2007, ASP Conf. Ser, 366, 158
- Steffen, J. H. et al. 2010, ApJ, 725, 1226
- Szabó, Gy. M., Szatmáry, K., Divéki, Zs. & Simon, A. 2006, A&A, 450, 395
- Szabó, Gy. M. et al. 2010, A&A, 523, A84
- Winn, J. N. et al. 2010, ApJ, 718, 575
- Young, A. T., 1967, AJ, 72, 747

This paper has been typeset from a \LaTeX file prepared by the author.